

Magnetic Structures of Thulium*

W. C. KOEHLER, J. W. CABLE, E. O. WOLLAN, AND M. K. WILKINSON
Oak Ridge National Laboratory, Oak Ridge, Tennessee

(Received January 24, 1962)

Neutron diffraction studies on polycrystalline and single-crystal specimens of thulium have been made at temperatures ranging from room temperature to 1.3°K. The results are interpreted by means of a method which exhibits explicitly the Fourier components of the distribution of magnetic moments on the lattice sites. At about 56°K, the Néel temperature, a simple oscillating z -component-type antiferromagnetic structure is developed. At approximately 40°K, nonzero Fourier coefficients of overtones of the fundamental observed at higher temperatures are first detected. At 4.2°K the magnetic structure of thulium is a type of antiphase domain structure in which several layers of moments parallel to the $+a_3$ direction are followed by several layers in which the moments are oppositely directed. The sequence in thulium is $-4, +3, -4, +3, \dots$ etc. Each atom has, within the precision of the experiments, an ordered moment of $7\mu_B$, and the ferrimagnetic structure has a net moment, parallel to the c axis, of $1\mu_B$ per atom. The fundamental period of the modulation remains constant over the whole range of temperatures at a value corresponding to 3.5 a_3 periods. In the course of this study the scattering amplitude of thulium was determined to be $b_{Tm} = (0.69 \pm 0.02) \times 10^{-12}$ cm.

INTRODUCTION

THE magnetic properties of polycrystalline thulium have been investigated by Rhodes, Legvold, and Spedding¹ and more recently by Davis and Bozorth.² The magnetic susceptibility at elevated temperatures follows a Curie-Weiss law: the slope of the $1/\chi$ vs T curve corresponds to the theoretical value of $\mu_{eff} = 7.56\mu_B$ for a $4f^{12}$ configuration ($L=5, S=1, J=6$). At a temperature variously reported as¹ 51°K or² 60°K there is observed a maximum in the susceptibility vs temperature curve which is attributed to a magnetic ordering transition to an antiferromagnetic state. Below about 20°K, ferromagnetism is detected, the Curie point for which is reported as 22°K. The highest moment observed, however, corresponds to about $0.5\mu_B$ per atom. The heat capacity of polycrystalline thulium³ shows a rather broad λ -type anomaly peaked near 55°K, but there is observed no additional anomaly in the neighborhood of the ferromagnetic Curie point.

In a study of the magnetization of polycrystalline thulium in very strong magnetic fields, up to 70 koe, Henry⁴ observed a saturation magnetization of $3.4\mu_B$ per atom at liquid helium temperatures which he interpreted as lending support for a $^2F_{3/2}$ ground state for thulium instead of the 3H_6 ground state characteristic of the tripositive ion.

The present investigation by neutron diffraction techniques has been undertaken to determine the magnetic structures of thulium in the several temperature regions as a first step in an attempt to understand the complex magnetic properties of this material.

POWDER DIFFRACTION STUDIES

The initial stages of the investigation of thulium were concerned with polycrystalline samples. Specimens of cast metal were obtained from commercial sources and diffraction samples were prepared by filing in an inert atmosphere. Diffraction patterns were obtained at temperatures ranging from room temperature to 1.3°K.

At room temperature, and at 78°K, the patterns were characteristic of the hexagonal close packed metal⁵ and there was no indication of long-range magnetic ordering. Below about 53°K there were observed additional coherent magnetic reflections some of which were found at positions slightly displaced from the nuclear reflections. A typical set of data taken at

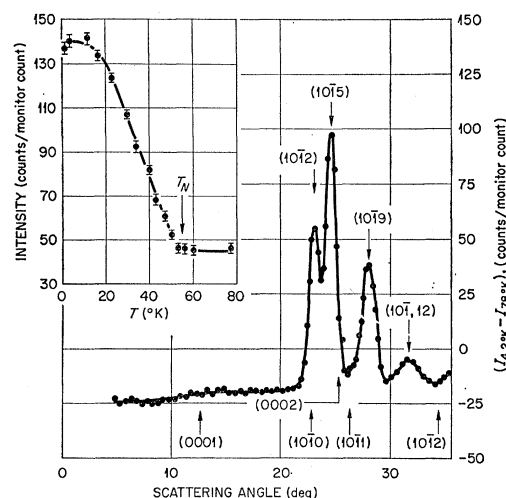


FIG. 1. Temperature difference pattern of thulium. The insert shows the variation with temperature of one of the prominent magnetic reflections.

* A brief account of portions of this work has been presented to the Seventh Annual Conference on Magnetism and Magnetic Materials, Phoenix, Arizona, November, 1961.

¹ B. L. Rhodes, S. Legvold, and F. H. Spedding, Phys. Rev. **109**, 1547 (1958).

² D. D. Davis and R. M. Bozorth, Phys. Rev. **118**, 1543 (1960).

³ L. D. Jennings, E. Hill, and F. H. Spedding, J. Chem. Phys. **34**, 2082 (1961).

⁴ W. E. Henry, J. Appl. Phys. **31**, 323S (1960).

⁵ In the course of this investigation, the hitherto unknown scattering amplitude for thulium has been measured as $b_{Tm} = 0.69 \pm 0.02 \times 10^{-12}$ cm. The sign is known to be positive from unpublished work in this laboratory on TmN.

4.2°K is shown in Fig. 1 where the magnetic scattering effects are displayed in a temperature difference pattern. In the portion of the pattern shown there are apparently four magnetic reflections. It is possible to index these reflections on the basis of a large magnetic cell, the c axis of which is seven times as long as that of the chemical cell. In this case the four reflections would be $(10\bar{1}2)$, $(10\bar{1}5)$, $(10\bar{1}9)$, and $(10\bar{1},12)$ as shown. It must be admitted that the identification of these reflections is subject to considerable uncertainty, particularly when such a large unit cell is required, and in view of the poor resolution inherent in powder data. Nevertheless, it was possible to conclude that there is a complex and probably antiferromagnetically ordered structure in thulium at 4.2°K. In addition, it appeared highly probable that the moments in the structure are parallel to the c axis since no magnetic reflections were observed inside the $(10\bar{1}0)$ nuclear peak. The powder data were considered to be sufficiently ambiguous as to preclude a more thorough analysis of the structure, but it was only when the single-crystal data, which are described in the next section, were obtained that the extent of this ambiguity was fully realized.

An important datum was obtained from the powder data in spite of the lack of detailed knowledge of the magnetic structure. From the analysis of the diffuse scattering in the temperature difference pattern, the effective ordered moment of thulium at 4.2°K was found to be $(6.8 \pm 0.4)\mu_B$, a value consistent with the paramagnetic susceptibility results, and with the value expected for the ordered tripositive ion.

The insert to Fig. 1 shows the temperature dependence of the magnetic reflection identified as $(10\bar{1}5)$. This is close to the $(10\bar{1}1)$ nuclear peak, and there is a sizeable nuclear contribution to the reflection as indicated. The Néel temperature, as measured from the intensity-temperature curve, is close to 53°K for this sample.

SINGLE-CRYSTAL STUDIES

A. Experimental Procedure

The single crystal used in the investigation was originally in the form of a pillar 12 mm long, 2 mm wide, and 2.3 mm thick. After preliminary orientation studies, the crystal was machined so that there were two flat surfaces perpendicular to the c axis, which surfaces were necessary for mounting the crystal in the low-temperature goniometer. After the machining, the crystal had an irregular shape so that absorption corrections could not readily or accurately be calculated. An alternative procedure for determining the absorption correction was therefore adopted.

The integrated intensity in a single-crystal reflection which is free of extinction may be represented by

$$E_{hkl} = KI_0 |F_{hkl}|^2 A_{hkl} / \sin 2\theta_{hkl}, \quad (1)$$

where K is a constant in any given experiment, I_0 is the

incident beam intensity, F_{hkl} is the structure factor per unit cell, θ_{hkl} is the Bragg angle for the reflection hkl , and A_{hkl} is the absorption function. If one rotates the crystal about the c axis so that a given $(10\bar{1}0)$ reflection, for example, is in position to reflect, one may obtain a series of reflections $(10\bar{1}l)$ and $(000l)$ by rotating the crystal about a vertical axis and by making the necessary adjustments in the counter position. If one knows the structure factors, one may measure directly the product $KI_0 A_{hkl}$ for each such reflection. A convenient parameter against which to plot these measured products is the angle φ which the c axis makes with the incident beam. A representative set of observations for the single-crystal specimen of thulium used in this investigation is shown in Fig. 2.

In this figure the values $KI_0 A_{hkl}$ were calculated from the nuclear intensities measured at 78°K, and from the experimentally observed value for b_{Tm} . A small temperature correction based on a Debye temperature obtained from the specific heat³ data has also been applied. It will be noted that when the crystal is so oriented around the c axis that the $(10\bar{1}l)$ reflections can be observed the absorption function is a minimum for (0002) but is changing rapidly with increasing φ . The absorption function levels off in the region of the $(10\bar{1}1)$ and $(10\bar{1}0)$ reflections. Since preliminary surveys of the magnetic reflections showed that the region between $(10\bar{1}0)$ and $(10\bar{1}1)$ was particularly significant and that the region around (0002) was devoid of magnetic reflections, the particular orientation shown was chosen for the quantitative measurements. For a given magnetic reflection, then, which occurs at a

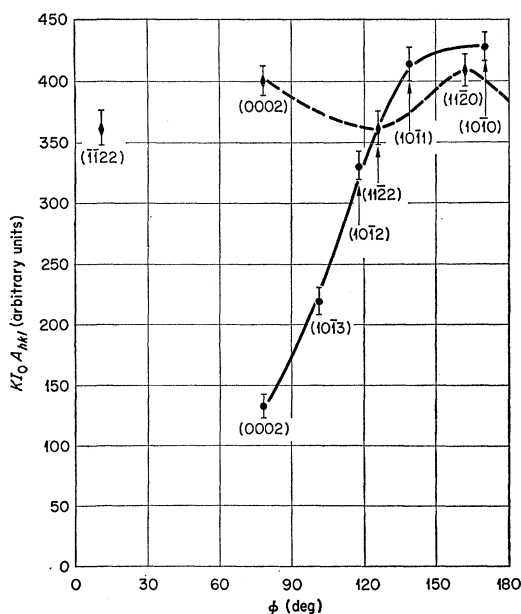


FIG. 2. Variation of the absorption function with crystal orientation. The angle φ is the angle which the c axis makes with the incident beam for various reflections.

value of φ between $(10\bar{1}1)$ and $(10\bar{1}0)$, the value of KI_0A_{hkl} is read from the curve, and the magnetic structure factor is evaluated in terms of this product, the angular function, and the observed intensity. Similarly, for a crystal orientation in which $(11\bar{2}l)$ reflections were to be observed, that orientation was chosen which gave the most favorable absorption function.

B. Description of the Diffraction Data and Analysis of the Structures

Having selected suitable orientations for the crystal, a series of systematic searches of portions of reciprocal space was made at various temperatures below the Néel temperature. By suitably coupling the crystal and counter motion, one may survey along radial lines passing through the origin, or alternatively, by fixing the counter and rotating the crystal one may search in circular arcs in reciprocal space. Ultimately the magnetic scattering density maps shown schematically in Fig. 3 were obtained.

In the upper portion of the figure, results for a sample temperature of 45°K are displayed. The reciprocal lattice points are shown as open, quartered, or full circles in order to represent the geometrical structure factors of the hexagonal close packed structure. If R is the geometrical structure factor, then $|R|^2=0, 1, 3$, or 4 is designated by open circles, those with one dark quarter, three dark quarters, or by full circles, respectively.

Associated with each allowed nuclear reflection is a single pair of symmetrically disposed magnetic reflections, or magnetic satellites, which lie on lattice rows parallel to the reciprocal lattice vector \mathbf{b}_3 with the

important exception that no satellites of $(000l)$ reflections are observed.

As shown in the Appendix, the existence of the single pair of magnetic satellites implies that there is a sinusoidal modulation of the magnetic scattering amplitude, the wave vector $\boldsymbol{\tau}$ of which is parallel to \mathbf{b}_3 . The absence of $(000l)$ satellites implies that the structure is a uniaxial one. One is thus forced to the conclusion that the magnetic structure of thulium at 45°K is the oscillating z -component type structure which has previously been reported for the high-temperature phase in erbium.⁶

The magnitude of the wave vector of the modulation can be measured from the separation of the satellites and it is found to be equal to $(2/7)\mathbf{b}_3$.

At 4.2°K, the distribution of magnetic scattering density in reciprocal space is much more complex. As in the high-temperature region, however, there are observed no magnetic satellites of $(000l)$ reflections, which again implies a uniaxial structure with moments aligned parallel or antiparallel to the a_3 direction. As one notes in the lower half of Fig. 3, there are observed magnetic satellites around $(11\bar{2}0)$, for example, at positions corresponding to $(4/7)\mathbf{b}_3$ and $(6/7)\mathbf{b}_3$ as well as at $(2/7)\mathbf{b}_3$. We take the point of view that $\boldsymbol{\tau}=(2/7)\mathbf{b}_3$ is the fundamental wave vector, and hence that the other two are the second and third harmonics. In the vicinity of $(10\bar{1}0)$ one finds satellites corresponding to $\boldsymbol{\tau}$, $2\boldsymbol{\tau}$, and $3\boldsymbol{\tau}$ as in the case mentioned above, but in addition there are satellites corresponding to $\bar{1}\boldsymbol{\tau}$, $\bar{2}\boldsymbol{\tau}$, and $\bar{3}\boldsymbol{\tau}$ or to wave vectors $(5/7)\mathbf{b}_3$, $(3/7)\mathbf{b}_3$, and $(1/7)\mathbf{b}_3$, respectively. It is to be emphasized that these latter three reflections do not appear in association with $(11\bar{2}0)$. This fact plays an important role in the analysis of the data.

The method of analysis which we have adopted for the low-temperature form of thulium is outlined in the Appendix. Starting from Eq. (A10) and writing explicitly $\mathbf{B}_H=\mathbf{b}_1+\mathbf{b}_2$, one finds that⁷

$$|\psi_p^0|^2 + |\psi_p^{\frac{1}{2}}|^2 + 2 \operatorname{Re} \psi_p^0 (\psi_p^{\frac{1}{2}})^* \exp(i2\pi \mathbf{t}_p \cdot \mathbf{a}_3/2) = 0 \quad (2)$$

must hold for $\mathbf{t}_p=(1/7)\mathbf{b}_3$, $(3/7)\mathbf{b}_3$, and $(5/7)\mathbf{b}_3$, corresponding to the absence of these satellites of $(11\bar{2}0)$.

If one writes for ψ_p^0 , $|\psi_p^0|$, $\exp(i\varphi_p^0)$, where φ_p^0 is a phase factor, and a similar expression for $\psi_p^{\frac{1}{2}}$, one has the following relation to be satisfied:

$$1 + |\psi_p^{\frac{1}{2}}|^2/|\psi_p^0|^2 + 2|\psi_p^{\frac{1}{2}}|/|\psi_p^0| \times \cos(2\pi \mathbf{t}_p \cdot \mathbf{a}_3/2 + \varphi_p^{\frac{1}{2}} - \varphi_p^0) = 0, \quad (3)$$

from which it follows that $|\psi_p^0| = |\psi_p^{\frac{1}{2}}|$ and

$$\varphi_p^0 - \varphi_p^{\frac{1}{2}} + 2\pi \mathbf{t}_p \cdot \mathbf{a}_3/2 = \pm\pi.$$

These relations obtained from the three absent satellites of $(11\bar{2}0)$ together with the general condition

⁶ J. W. Cable, E. O. Wollan, W. C. Koehler, and M. K. Wilkinson, J. Appl. Phys. **32**, 49S (1961).

⁷ The symbols in this equation and those to follow are defined in the Appendix.

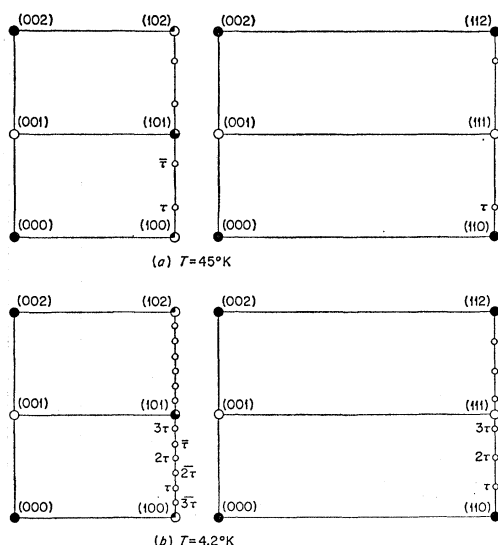


FIG. 3. Schematic representation of diffraction effects in thulium at 45°K and at 4.2°K.

TABLE I. Relative phases of Fourier amplitudes for the sites (0,0,0) and (1/3,2/3,1/2) as determined from the observation of systematic absences.

\mathbf{t}_p	$\psi_p^0/\psi_p^{\frac{1}{2}}$	\mathbf{t}_p	$\psi_p^0/\psi_p^{\frac{1}{2}}$
(1/7) \mathbf{b}_3	$\exp[i2\pi(3/7)]$	(6/7) \mathbf{b}_3	$\exp[-i2\pi(3/7)]$
(3/7) \mathbf{b}_3	$\exp[i2\pi(2/7)]$	(4/7) \mathbf{b}_3	$\exp[-i2\pi(2/7)]$
(5/7) \mathbf{b}_3	$\exp[i2\pi(1/7)]$	(2/7) \mathbf{b}_3	$\exp[-i2\pi(1/7)]$

$(\psi_p^k) = (\psi_{-p}^k)^*$ serve to fix the relative phases of ψ_p^0 and $\psi_p^{\frac{1}{2}}$, and these are listed in Table I. With these values the intensity J_p may be written

$$J_p = A^2 N \sin^2 \theta |\psi_p^0|^2 [2 \pm 2 \cos(2\pi \mathbf{B}_H \cdot \mathbf{r})], \quad (4)$$

where the positive sign is to be taken for $\mathbf{t}_p = (2/7)\mathbf{b}_3$, $(4/7)\mathbf{b}_3$, and $(6/7)\mathbf{b}_3$, and the negative sign for $\mathbf{t}_p = (1/7)\mathbf{b}_3$, $(3/7)\mathbf{b}_3$, and $(5/7)\mathbf{b}_3$.

Measurements of the intensities of the various satellite reflections can thus be reduced to the magnitudes of the Fourier coefficients provided the form factor is known. We have evaluated the form factor at the points of interest by a series of successive approximations, for the first of which we have used the appropriately scaled form factor for trivalent erbium.⁸

In Table II are listed the observed values⁹ of $|F|_{\text{mag}}^2$ for the several satellite reflections of three important nuclear reflections together with the corresponding values of $|\psi_p^0|/\sqrt{7}$. For each amplitude there are four distinct determinations, and it will be noted that the agreement is generally excellent. The average values are given in the lower part of the table.

In addition to the scattering J_p , there is also found, at 4.2°K, a small but measurable magnetic contribution to some of the normal lattice reflections. It is observed further that there are no magnetic contributions to reflections (000 l) or to (1121). The first of these observations implies that the mean moments of the two sets of sites are parallel to the a_3 direction: the second, that the mean moments are equal in magnitude and direction, as may be seen by reference to Eq. (A11). The Laue-Bragg scattering J_1 can thus be expressed as

$$|\bar{F}|_{hkl}^2 = \frac{J_1}{N^2} = A^2 \sin^2 \theta \frac{|\psi_0^0|^2}{N} [2 + 2 \cos(2\pi \mathbf{B}_H \cdot \mathbf{r})]. \quad (5)$$

This last expression serves to measure the coefficient $|\psi_0^0|$. In Table II the average value of this coefficient as obtained from four reflections is listed with the average values of $|\psi_p^0|$. Within the error of observation, the mean moment per atom is $1.0\mu_B$.

In order to synthesize the moment distribution, one needs the phases of the Fourier coefficients as well as their magnitudes. In general, the phases are not determined experimentally. In this case, however, a unique structure can be derived.

⁸ W. C. Koehler and E. O. Wollan, Phys. Rev. **92**, 1380 (1953).

⁹ As here used the symbol $|F|_{\text{mag}}^2$ is equal to J_p/N^2 , e.g., J_p referred to a unit chemical cell.

It may be assumed that the maximum value which the moment on any atom may take is approximately $7\mu_B$. Since it is known from the diffuse scattering measurements on polycrystalline thulium that the average moment per atom is nearly $7\mu_B$, it follows that the moment at each lattice site must also be approximately $7\mu_B$. It further follows that these must be distributed on each set of sites so that there is a net moment of $1\mu_B$.

With the experimentally determined values of the magnitudes of the Fourier coefficients, the series representation for the moments on the $k=0$ sites [Eq. (A6)] may be written

$$\begin{aligned} \mu_0^L/\mu_B = & -1.0 + 9.0 \cos[2\pi(2/7)L + \theta_1] \\ & + 2.2 \cos[2\pi(4/7)L + \theta_2] \\ & + 3.2 \cos[2\pi(6/7)L + \theta_3], \quad (6) \end{aligned}$$

where the negative sign for $|\psi_0^0|$ has been taken for convenience and θ_1 , θ_2 , and θ_3 are the phase angles of the coefficients ψ_1^0 , ψ_2^0 , and ψ_3^0 , respectively.

The condition to be satisfied by the phase angles θ_i is that the magnitude of the magnetic moment be $7\mu_B$ for every L . For $L=0$ one sees by inspection that the set of phases $\theta_1=0$, $\theta_2=0$, and $\theta_3=\pi$ satisfies the condition. With this choice of phases and the set of relative phases given in Table I, a structure can be generated. (Clearly other sets of phases for $L=1, 2, \dots$, etc., may be written down but these correspond merely to relabelling the lattice sites and are not distinct solutions.)

The magnetic structure so derived is represented in Fig. 4. With the choice of origin shown in the figure the sequence for the $k=0$ sites is $+-+--$; for the

TABLE II. Magnetic intensities of magnetic reflections of thulium at 4.2° and corresponding normalized Fourier amplitudes.

Reflection	$ F _{\text{mag}}^2$ (10^{-24} cm ² /unit cell ²) (observed)	$ \psi_p^0 /\sqrt{7}$
(1120)	0.16 \pm 0.06	1.02
τ	2.94 \pm 0.2	4.42
2τ	0.17 \pm 0.015	1.06
3τ	0.36 \pm 0.025	1.61
(1121)	0.0	
3τ	0.33 \pm 0.025	1.58
2τ	0.13 \pm 0.02	1.06
1τ	2.19 \pm 0.16	4.60
(1122)	0.10 \pm 0.06	1.05
(1010)	0.061 \pm 0.02	1.03
3τ	0.421 \pm 0.02	1.58
τ	1.14 \pm 0.07	4.53
2τ	0.189 \pm 0.01	1.09
2τ	0.069 \pm 0.005	1.17
1τ	2.79 \pm 0.15	4.42
3τ	0.123 \pm 0.02	1.68
(1011)	0.14 \pm 0.05	1.06
$\langle \psi_0^0 \rangle / \sqrt{7} = 1.04$; $\langle \psi_1^0 \rangle / \sqrt{7} = 4.50$; $\langle \psi_2^0 \rangle / \sqrt{7} = 1.10$; $\langle \psi_3^0 \rangle / \sqrt{7} = 1.61$.		

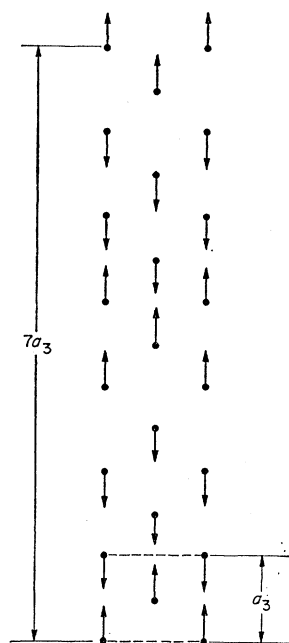


FIG. 4. Magnetic structure of thulium at 4.2°K.

$k=\frac{1}{2}$ sites, it is $+-+--+-+$, and this results in an over-all $-4, +3, -4, +3, \dots$ arrangement.¹⁰

That this structure is unique can be shown in a number of ways, of which we consider one. We need consider the distribution on only one of the sets of sites, the $k=0$ set, for example. As a result of the severe limitations on possible structures imposed by the experimental results, we have to consider a combinatorial problem in which it is required to place four objects (south pointing moments) in seven boxes (the lattice sites). Of the 35 possible arrangements only five need be considered; the remaining 30 can be derived from them by cyclic permutation, e.g., by relabelling the lattice sites. These configurations are listed in Table III together with the values of $|\psi_p^0|$ calculated from them. It may be seen that only the

TABLE III. Comparison of Fourier amplitudes calculated for the five possible configurations with experiment. The configurations shown are for $k=0$ sites only. The configurations for the $k=\frac{1}{2}$ sites may be obtained by shifting those given by three $\frac{1}{2}a_3$ spacings. Of the five possibilities, configuration number 3 gives the closest possible approach to an antiphase domain structure. Configurations 2 and 5 are indistinguishable insofar as diffraction effects are concerned.

Configuration	$ \psi_1^0 /\sqrt{7}$	$ \psi_2^0 /\sqrt{7}$	$ \psi_3^0 /\sqrt{7}$
1. $+++----$	1.11	1.60	4.49
2. $+-+--+-$	2.83	2.83	2.83
3. $+-+--+-$	4.49	1.11	1.60
4. $+-+--+-$	1.60	4.49	1.11
5. $+-+--+-$	2.83	2.83	2.83
Observed	4.50	1.10	1.61

¹⁰ Configurations which have the signs of all spins reversed may also exist, and will be indistinguishable insofar as diffraction effects are concerned from that described.

configuration number 3, corresponding to the one described above, gives satisfactory agreement with experiment.

C. Temperature Dependence of the Fourier Coefficients

The variation with temperature of the intensities of representative magnetic reflections of thulium is shown in the left side of Fig. 5. On the right side is shown the variation with temperature of the magnitudes of the corresponding Fourier coefficients. As the temperature is reduced to the Néel temperature, in this case about 56°K, the intensity of the primary satellite of $(11\bar{2}0)$ increases sharply and approaches its saturation value at about 20°K. Only the primary satellites are observed until a temperature near 40°K is reached, at which point the second and third harmonics make their appearance. The intensities of the higher harmonics appear to be saturated at 4.2°K. The magnetic contributions to the normal reflections $(11\bar{2}0)$ and $(10\bar{1}0)$ set in at a temperature which is difficult to determine with high precision.

The temperature variation of $|\psi_0^0|$ also is represented in Fig. 5 but it must be emphasized that the precision of this quantity is very low in comparison with that of the other Fourier coefficients.

DISCUSSION

By a combination of powder and single-crystal neutron diffraction studies we have determined the magnetic structures of thulium in the temperature range above 40°K and at 4.2°K.

The oscillating z -component structure which sets in just below the Néel temperature can be expected to be stable whenever the anisotropy is such as to produce moments parallel to the a_3 direction.¹¹⁻¹³ In the case of thulium, all orders of the anisotropy energy select the a_3 direction as the preferred axis.^{11,13} In the approximation that only exchanges between first and second neighbor layers need be considered, the energy of the oscillatory model is minimized when $\cos(2\pi\tau \cdot \mathbf{a}_3/2) = -A_1/4A_2$ in which A_1 and A_2 are the corresponding exchange parameters. As Elliott has emphasized, the energy of the ferromagnetic state is lower than that of the oscillatory state, but by virtue of its increased entropy, the oscillatory state has the lower free energy.

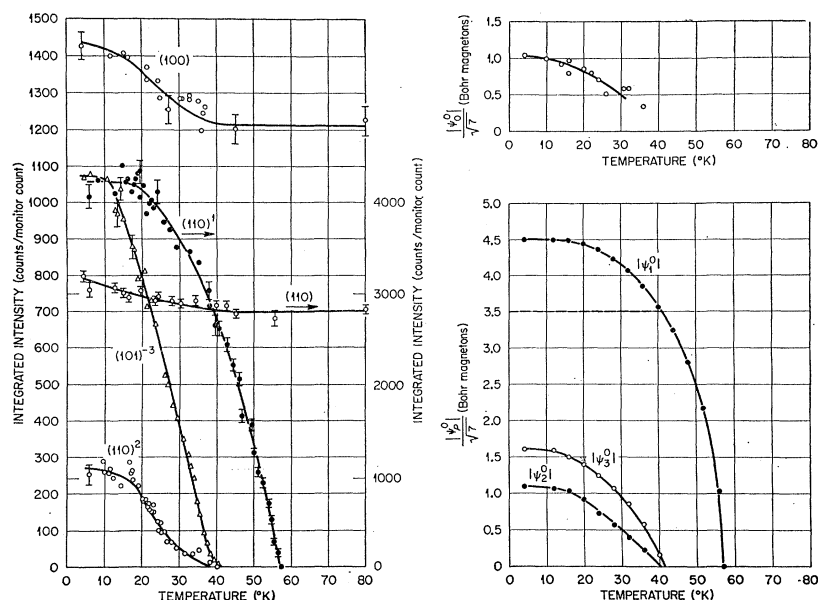
The oscillating component model can persist only to that temperature at which the moment saturates. In thulium this occurs, as shown in the right-hand side of Fig. 5, at about 40°K as indicated by the dashed line corresponding to a value of $|\psi_1^0|/\sqrt{7} = 3.5\mu_B$. It is at this temperature that a transformation to another structure must occur and this transformation is

¹¹ R. J. Elliott, Phys. Rev. **124**, 346 (1961).

¹² T. A. Kaplan, Phys. Rev. **124**, 329 (1961).

¹³ H. Miwa and K. Yosida, Proceedings of the International Conference on Magnetism and Crystallography, Kyoto, Japan, September, 1961 (unpublished).

FIG. 5. Temperature variations of magnetic reflections and Fourier amplitudes in thulium. The dashed line in the right-hand side of the figure corresponds to the maximum value which the normalized coefficient $|\psi_0^0|$ may take in the oscillatory structure. Arrows in the left-hand side of the figure indicate that the scale at the right is to be used.



evidenced by the appearance of overtones of the fundamental modulating frequency.

The structure which is found at low temperature can be envisaged as an antiphase-domain-type structure in which several layers of south-pointing moments are followed by several layers of north-pointing moments. The particular antiphase-domain structure which occurs is unusual in that it is ferrimagnetic. We have accordingly dwelt on the demonstration of its uniqueness at some length.

The net moment of $1.0\mu_B$ which has been derived from the diffraction data is entirely consistent with the results of the low-field measurements of Davis and Bozorth² when one takes into consideration the fact that their measurements were made with polycrystalline samples. The measurements of Henry⁴ are now to be understood as showing evidence for a field-induced transformation, setting in at about 13 koe to a c -axis ferromagnet. The magnetization of $3.4\mu_B$ observed at 70 koe is to be attributed, as first suggested by Davis and Bozorth, to a very high axial anisotropy. The breadth of the λ anomaly in the specific heat data is presumably associated with the transition at about 40°K.

It is unfortunately not possible to say definitely that the low-temperature structure persists up to 40°K. In view of the Curie point measurement of 22°K, it would in fact appear that the net moment should be absent above that temperature. Reference to the curves of Fig. 5 shows, however, that even at 30°K the Fourier coefficients of the fundamental and of its harmonics are sufficiently saturated as to require the ferrimagnetic structure. Only in a narrow temperature range near 40°K can an antiferromagnetic configuration be constructed. It is probable, but by no means established, that the coefficient $|\psi_0^0|$ first appears near 40°K rather than at 22°K.

ACKNOWLEDGMENTS

It is a great pleasure for the authors to express their gratitude to Professor Sam Legvold and Professor F. H. Spedding and their students for providing them with their single-crystal specimen. J. McWane and H. R. Child have contributed to this work in the collection and processing of data. Their assistance is gratefully acknowledged.

APPENDIX

It has been pointed out that the intensity formula necessary for the interpretation of neutron diffraction data from helical spin structures⁸ may be derived in a simple way by the application of the general theory of x-ray scattering from disordered lattices as given by Zachariasen.¹⁴ We take the same point of view here to calculate intensity relations for the simple oscillating component type magnetic structure and to give a useful interpretation to the low-temperature data of thulium in which are observed the higher order satellites. In the notation of our earlier discussion,⁸ the intensity of scattering from a small crystallite may be written as a sum of two terms, $I = J_1 + J_2$, with

$$J_1 = |\bar{F}|^2 \sum_{L, L'} \exp[i\mathbf{s} \cdot (\mathbf{A}_L - \mathbf{A}_{L'})],$$

$$J_2 = \sum_{L, L'} \exp[i\mathbf{s} \cdot (\mathbf{A}_L - \mathbf{A}_{L'})] \times \sum_{k, k'} \varphi_{k, k'}^{L-L'} \exp[i\mathbf{s} \cdot (\mathbf{r}_k - \mathbf{r}_{k'})]. \quad (A1)$$

The first term, J_1 , gives the Laue-Bragg scattering at the reciprocal lattice points, and is proportional to the absolute square of the mean structure factor. The second

¹⁴ W. H. Zachariasen, *Theory of X-Ray Diffraction in Crystals* (John Wiley & Sons, Inc., New York, 1945), Chap. 4.

term, J_2 , is usually called the disorder scattering.¹⁵ In this term, the quantity $\varphi_{k,k'}^M$ is a correlation function given by

$$\varphi_{k,k'}^M = \frac{1}{N} \sum_L \varphi_k^L \cdot (\varphi_{k'}^{L-M})^* \quad (\text{A2})$$

If \mathbf{p}_k^L is the magnetic scattering amplitude of the atom located at the site $\mathbf{r}_k + \mathbf{A}_L$, where \mathbf{A}_L is a lattice vector and \mathbf{r}_k is the position vector within a unit chemical cell, and $\langle \mathbf{p}_k \rangle$ is the mean scattering amplitude of the set k , the deviations from the mean of the amplitudes φ_k^L may be expressed as $\varphi_k^L = \mathbf{p}_k^L - \langle \mathbf{p}_k \rangle$. The quantity $\varphi_{k,k'}^M$ in Eq. (A2) represents the mean product of deviations for sites separated by $\mathbf{r}_k - \mathbf{r}_{k'} + \mathbf{A}_L - \mathbf{A}_{L'}$. In what follows we shall be concerned with structures in which the deviations are doubly periodic, e.g., we shall assume that there exist planes normal to a reciprocal lattice vector $\boldsymbol{\tau}$ in which the magnetic moments are parallel.

A. Oscillating Component Model

For an oscillating component model, the components of the moments parallel to some direction \hat{u}_3 are supposed to vary sinusoidally with distance along $\boldsymbol{\tau}$. No order is assumed for the perpendicular components. The moment distribution may be described by

$$\mu_k^L \hat{u}_3 = (\mu_{\max}/2) \{ \exp[i2\pi\boldsymbol{\tau} \cdot (\mathbf{r}_k + \mathbf{A}_L)] + \text{c.c.} \} \hat{u}_3. \quad (\text{A3})$$

(An arbitrary phase factor should be introduced but it is not included since it does not appear in the intensity.)

The correlation function for such a structure has the form

$$\varphi_{k,k'}^M = \frac{1}{4} (e^2 \gamma f_e / 2mc^2)^2 \mu_{\max}^2 \sin^2 \theta \times \{ \exp[i2\pi\boldsymbol{\tau} \cdot (\mathbf{r}_k - \mathbf{r}_{k'} + \mathbf{A}_M)] + \text{c.c.} \}, \quad (\text{A4})$$

in which θ is the angle between the unit vector \hat{u}_3 and the scattering vector \mathbf{s} , f_e is the form factor, and all other symbols have their usual significance. The intensity J_2 may then be written, with the abbreviation $A = e^2 \gamma f_e / 2mc^2$,

$$J_2^{\pm} = \frac{1}{4} A^2 \mu_{\max}^2 \sin^2 \theta |R|^2 \prod_i \frac{\sin^2[\frac{1}{2}(\mathbf{s} \pm 2\pi\boldsymbol{\tau}) \cdot N_i \mathbf{a}_i]}{\sin^2[\frac{1}{2}(\mathbf{s} \pm 2\pi\boldsymbol{\tau}) \cdot \mathbf{a}_i]}, \quad (\text{A5})$$

$$J_2^{\pm} = \frac{1}{4} N^2 A^2 \mu_{\max}^2 \sin^2 \theta |R|^2, \quad \mathbf{s} = 2\pi(\mathbf{B}_H \pm \boldsymbol{\tau}).$$

This relation, in which $|R|^2$ is the square of the geometrical structure factor, shows that the scattering J_2 is zero unless $\mathbf{s} = 2\pi(\mathbf{B}_H \pm \boldsymbol{\tau})$, where $\mathbf{B}_H = h_1 \mathbf{b}_1 + h_2 \mathbf{b}_2 + h_3 \mathbf{b}_3$ is a reciprocal lattice vector. The magnetic scattering manifests itself in the form of satellites of the allowed nuclear reflections. With each allowed nuclear reflection is associated a single pair of magnetic satellites on reciprocal lattice rows parallel to $\boldsymbol{\tau}$. It will be noted

¹⁵ The magnetic structures in which we are interested here are, strictly speaking, triply periodic, and the designation of J_2 as disorder scattering is inappropriate. It is nevertheless convenient to retain the framework developed for disordered crystals, because in many cases the magnetic cell is incommensurate with the chemical cell, and moreover it may vary with temperature.

that, contrary to the case for helical spin structures, extinctions of otherwise allowed satellites will occur when $\sin \theta$ can be zero.

Inspection of the data for the high-temperature form of thulium shows that $\boldsymbol{\tau}$ is parallel to \mathbf{b}_3 . Since $\sin \theta$ is zero for reflections (000*l*), \hat{u}_3 is also parallel to \mathbf{b}_3 .

B. "Squared Up" Structure

The moment distribution for each set of sites k may be expanded in a Fourier series

$$\begin{aligned} \mathbf{u}_k^L &= \frac{1}{\sqrt{N}} \sum_p \boldsymbol{\psi}_p^k \exp(i2\pi \mathbf{t}_p \cdot \mathbf{A}_L), \\ \mathbf{u}_p^k &= \frac{1}{\sqrt{N}} \sum_L \mathbf{u}_k^L \exp(-i2\pi \mathbf{t}_p \cdot \mathbf{A}_L), \end{aligned} \quad (\text{A6})$$

where we may choose

$$\mathbf{t}_p = (p_1/N_1)\mathbf{b}_1 + (p_2/N_2)\mathbf{b}_2 + (p_3/N_3)\mathbf{b}_3, \quad 0 \leq p_i < N_i. \quad (\text{A7})$$

In terms of the Fourier coefficients, the correlation $\varphi_{k,k'}^M$ becomes

$$\varphi_{k,k'}^M = \frac{A^2}{N} \sum_{p \neq 0} [\boldsymbol{\psi}_p^k \cdot (\boldsymbol{\psi}_p^{k'})^* - (\mathbf{s} \cdot \boldsymbol{\psi}_p^k)(\mathbf{s} \cdot \boldsymbol{\psi}_p^{k'})^*] \times \exp[i2\pi \mathbf{t}_p \cdot (\mathbf{A}_L - \mathbf{A}_{L'})], \quad (\text{A8})$$

and the intensity J_2 takes the form

$$\begin{aligned} J_p &= A^2 N \sum_{k,k'} [\boldsymbol{\psi}_p^k \cdot (\boldsymbol{\psi}_p^{k'})^* - (\mathbf{s} \cdot \boldsymbol{\psi}_p^k)(\mathbf{s} \cdot \boldsymbol{\psi}_p^{k'})^*] \\ &\quad \times \exp[i\mathbf{s} \cdot (\mathbf{r}_{k'} - \mathbf{r}_k)], \quad (\text{A9}) \end{aligned}$$

The intensity J_2 will now be found in a series of satellites of the reciprocal lattice points on lattice rows parallel to the vectors \mathbf{t}_p . The intensity of the p 'th satellite depends upon the coefficients of the p 'th Fourier waves in the moment distributions.

The term $p=0$ is excluded from the intensity J_2 because $\boldsymbol{\psi}_0^k = N^{\frac{1}{2}} \langle \mathbf{u}_k \rangle$. If $\boldsymbol{\psi}_0^k$ is different from zero it will contribute to the Laue-Bragg scattering J_1 .

For thulium at low temperatures, inspection of the data shows that the vectors \mathbf{t}_p are parallel to \mathbf{b}_3 , and that the moments have z components only. With the indices $k=0$ and $k=\frac{1}{2}$ to denote the lattice sites (0,0,0) and $(\frac{1}{3}, \frac{2}{3}, \frac{1}{2})$, respectively, and with $\mathbf{r} = \frac{1}{3}\mathbf{a}_1 + \frac{2}{3}\mathbf{a}_2 + \frac{1}{2}\mathbf{a}_3$, the function J_2 takes the simple form

$$J_p = A^2 N \sin^2 \theta \{ |\boldsymbol{\psi}_p^0|^2 + |\boldsymbol{\psi}_p^{\frac{1}{2}}|^2 + 2 \operatorname{Re}[\boldsymbol{\psi}_p^0 \boldsymbol{\psi}_p^{\frac{1}{2}*}] \times \exp(i2\pi(\mathbf{B}_H \cdot \mathbf{r} + \mathbf{t}_p \cdot \mathbf{a}_3/2)) \}. \quad (\text{A10})$$

The Laue-Bragg scattering for the same case becomes

$$\begin{aligned} |\bar{F}|^2 &= J_1/N^2 = A^2 \sin^2 \theta [\langle \mu_0 \rangle^2 + \langle \mu_1 \rangle^2 \\ &\quad + 2\langle \mu_0 \rangle \langle \mu_1 \rangle \cos(2\pi \mathbf{B}_H \cdot \mathbf{r})], \end{aligned} \quad (\text{A11})$$

where the observation that reflections (000*l*) have no magnetic contribution is expressed by the factor $\sin^2 \theta$.